Analysis of Fouling in HVAC Heat Exchangers by CFD

Jafari Nasr, Mohammad Reza*[+]

Research Institute of Petroleum Industry (RIPI), Tehran, I.R. IRAN

Balaei, Aida

Department of Chemical Engineering, Islamic Azad University, Science and Research Branch, Tehran, I.R. IRAN

ABSTRACT: *The purpose of this study is to identify parameters influence on the particle deposition within fin and tube heat exchanger of air-conditioning systems by CFD analysis. First the basic sketch of periodic geometry drawn and meshing operation including boundary conditions was performed. Then the gas side properties and flow parameters were solved by ANSYS Fluent 14.5 software. Lagrangian equations used for modeling dispersed phase and effect of injecting various particle sizes evaluated by Rosin-Rammler model. Moreover turbulence effect was investigated using discrete random walk model. Consequently it is observed that deposition rate is highly affected by particles diameter in which leads to 90% deposition for particles over 30 µm in diameter.*

KEY WORDS: *HVAC; Particle deposition; ANSYS fluent software; Lagrangian equation.*

INTRODUCTION

Air quality in many buildings plays an important role in residents' comfort and is directly affected by particles entered the building by channels, doors, windows; furthermore these particles affect the health of occupants significantly. Due to existence of humidity, bio-agents such as bacteria and fungi, could form colonies on the surfaces of Heating, Ventilation and Air Conditioning (HVAC) heat exchangers; not only have negative impact on residents' health, but also results in particle deposition, pressure drop and decreasing air-conditioning system efficiency. Therefore identification particles properties and deposition mechanism could lead to better design of HVAC systems [1].

Heat exchangers are the main part of every heating and cooling system. HVAC systems, as a heat exchanger, are being used in many buildings all around the world for air ventilation and conditioning. It is estimated that most of HVAC's are become fouled after 4 to 9 years depend on the applications. Therefore, it is important to understand and analyze their properties and characteristics [2].

Particle deposition would occur on surfaces of HVAC heat exchangers and cause inefficiencies in heat transfer and leads to pressure drop [3]. Furthermore existence of moisture not only causes surface corrosion because of chemical reactions, but also allows growth of bacteria and fungi on the surfaces which influence the indoor air quality and occupants residents' health [4].

Fin and tube heat exchangers are commonly used in HVAC systems. They comprised of horizontal tubes with air flow perpendicular to tubes and fins are extended vertically. The refrigerant flows through the tubes in cooling systems and the fins are mostly corrugated

* *To whom correspondence should be addressed.*

+ E-mail: nasrmrj@ripi.ir

1021-9986/15/3/51 *10/$/3.00*

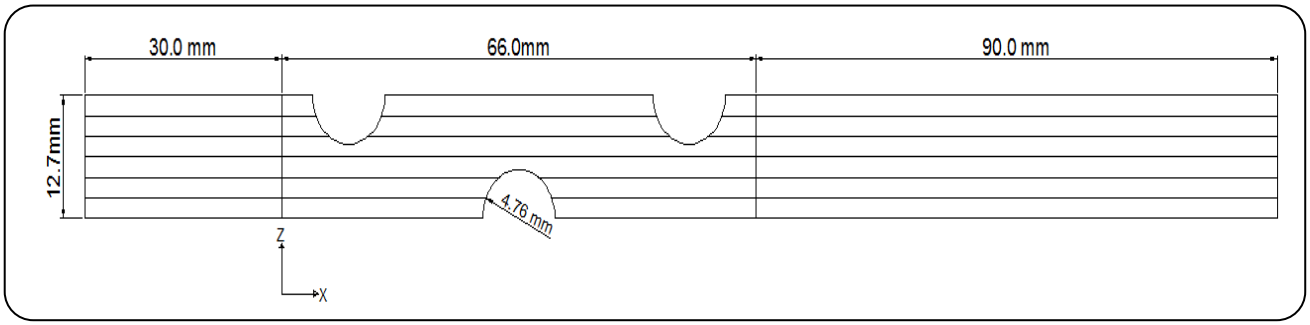

Fig. 1: Schematic view of extended computational domain.

to increase heat transfer to the air flow [5]. The air side heat transfer resistance often determines the performance of the fin and tube heat exchangers due to the lower heat transfer coefficient of air side rather than the refrigerant side [6]. Therefore to enhance the overall heat transfer, active and passive techniques are applied in many industries in order to increase the heat transfer coefficient either by external forces or special surfaces [7]. To designers, number of fins, tube rows and fin spacing are mostly main parameters to obtain the desire efficiency. However, pressure drops would be considered as main constraints [8]. Moreover, efforts to improve the prediction of fouling time would greatly benefit from more detailed information about large particle (>10μ m) concentration indoor air.

The purpose of this study is to evaluate particulate fouling occurs in HVAC heat exchangers, by Rosin-Rammler method which indicates the effect of particle injection with various particle diameters. This analysis performed by CFD (ANSYS Fluent V.14.5) software to clarify fouling mechanism and effective parameters involve in this phenomenon.

THEORITICAL SECTION

Model development

Model description

The experimental heat exchanger is common HVAC heat exchanger with 0.3048m × 0.3048m (12"×12") fin and tube heat exchanger with corrugated fins which contains two rows of tubes with an offset tube in the middle. As mentioned the fins are standing in vertical direction and tubes are located in horizontal direction while the air flow is perpendicular to the tubes. The thicknesses of fins and tube walls are neglected in this modeling. The refrigerant flows thorough the tubes in 4°C. The computational domain is considered the volume between the midpoints of one row of tubes and extended to the midpoint of the immediate offset row of tubes in vertical direction. The 3D geometry has 0.066m length and 0.0127 m height with fin spacing of 0.003175 m.

The Reynolds number of flow is calculated to be 2300 and this means the flow is transition, and the value of y^+=1 is achieved for near wall meshing due to flow conditions. After gas side meshing, the domain was extended from both sides of fins about half of the fin thickness in y-direction, moreover the model was extended 30 mm at the inlet to let the flow to be fully developed and 90 mm for eliminating effects of reversed flow and low pressure zones as seen in Fig. 1.

The computational domain was divided into smaller domains to promote meshing quality [9], and meshed by hexahedral cells. The meshing procedure was done till meshing independence confirmed and the total mesh number of 537600 was reported. Fig. 2 depicts the hexahedral meshing of gas side volume.

Boundary conditions

After the gas side of the heat exchanger was meshed, symmetry boundary conditions were assumed for both side of domain in z-directions. The following boundary conditions are given as followed [10];

$$\frac{\partial u}{\partial z} = \frac{\partial v}{\partial z} = 0 \ , \ \ w = 0 \ , \ \frac{\partial T}{\partial z} = 0 \qquad (1)$$

Also, the symmetry boundary conditions considered for top and bottom parts of the domain in y-directions as expressed in Eq. (2);

$$\frac{\partial T}{\partial y} = 0 \qquad (2)$$

The walls in the domain assumed without any resistivity and roughness. Furthermore the velocity profile was specified on the inlet and outlet of the boundary.

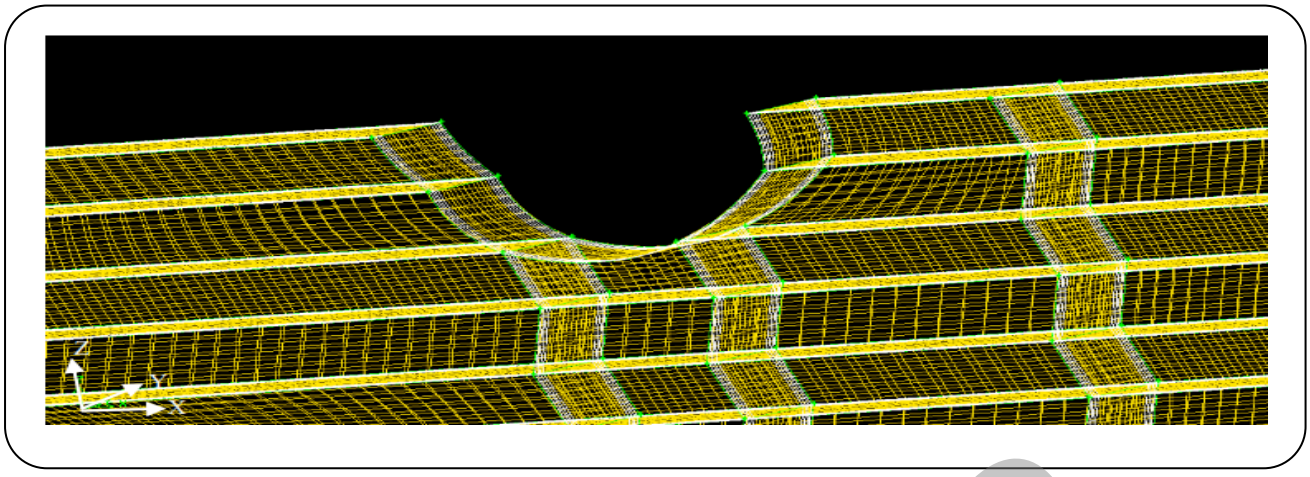

Fig. 2. Hexahedral meshing of gas side volume.

Fluid properties

The fluid assumed as a mixture of dry air and water vapor which modeled as inert material without any mass transfer. The density and viscosity of the fluid are expressed by ideal gas and Sutherland equations are considered as below [10];

$$\rho = \frac{p}{RT\left(\sum_m \frac{Y_m}{M_m}\right)} \tag{3}$$

$$\mu = \left(\frac{T}{273.15}\right)^{3/2}\left(\frac{273.15+C_s}{T+C}\right)\mu_0 \tag{4}$$

The refrigerant fluid assumed to have constant temperature of 4 ^{0}C; however the air inserted to the domain with a velocity and temperature of 1 m/s and 26.6 ^{0}C respectively. To simplify equations, the tube wall thicknesses were also neglected.

Governing equation

Conservation equations

The general equations for mass, momentum and energy conservations can be solved for the incompressible ideal gas with constant properties.

The conservation equation of mass is given as followed [10];

$$\frac{\partial p}{\partial t} + \frac{\partial}{\partial x_j}\left(\rho u_i\right) = s_m \tag{5}$$

The conservation equation of momentum is given by the following equation;

$$\frac{\partial p}{\partial t} + \frac{\partial}{\partial x_j}\left(\rho u_j u_{i-\tau_{ij}}\right) = -\frac{\partial p}{\partial x_i} + s_i \tag{6}$$

By applying static thermal enthalpy equation, the heat transfer issue, expressed in Eq. (7), would be solved.

$$\frac{\partial \rho h_t}{\partial t} + \frac{\partial}{\partial x_j}\left(\rho h_t u_j + F_{h_{t,j}}\right) = \frac{\partial \rho}{\partial t} + u_j\frac{\partial \rho}{\partial x_j} + s_h - \sum_m H_m s_{cm} \tag{7}$$

Mass transfer of fluid mixture

The mass transfer equation of the fluid mixture is defined as in Eq. (8);

$$\frac{\partial}{\partial t}\left(\rho Y_m\right) + \frac{\partial}{\partial x_j}\left(\rho u_j Y_m + F_{m,j}\right) = s_m \tag{8}$$

Conjugate heat transfer

Due to temperature variations between the solid and the air, conjugate heat transfer would be appropriated for solving temperature distribution according to the properties of material, flow and heat source. As pointed before, the thicknesses of fins and tube walls are neglected in this modeling. The conjugate heat transfer can be obtained by the Eq. (9) [10];

$$\frac{\partial\left(\rho e\right)}{\partial t} = \frac{\partial}{\partial x_i}\left(k\frac{\partial T}{\partial x_i}\right) + s_e \tag{9}$$

Flow conditions in fluent

The fluid consists of dry air as an incompressible ideal gas including water vapor as inert material which

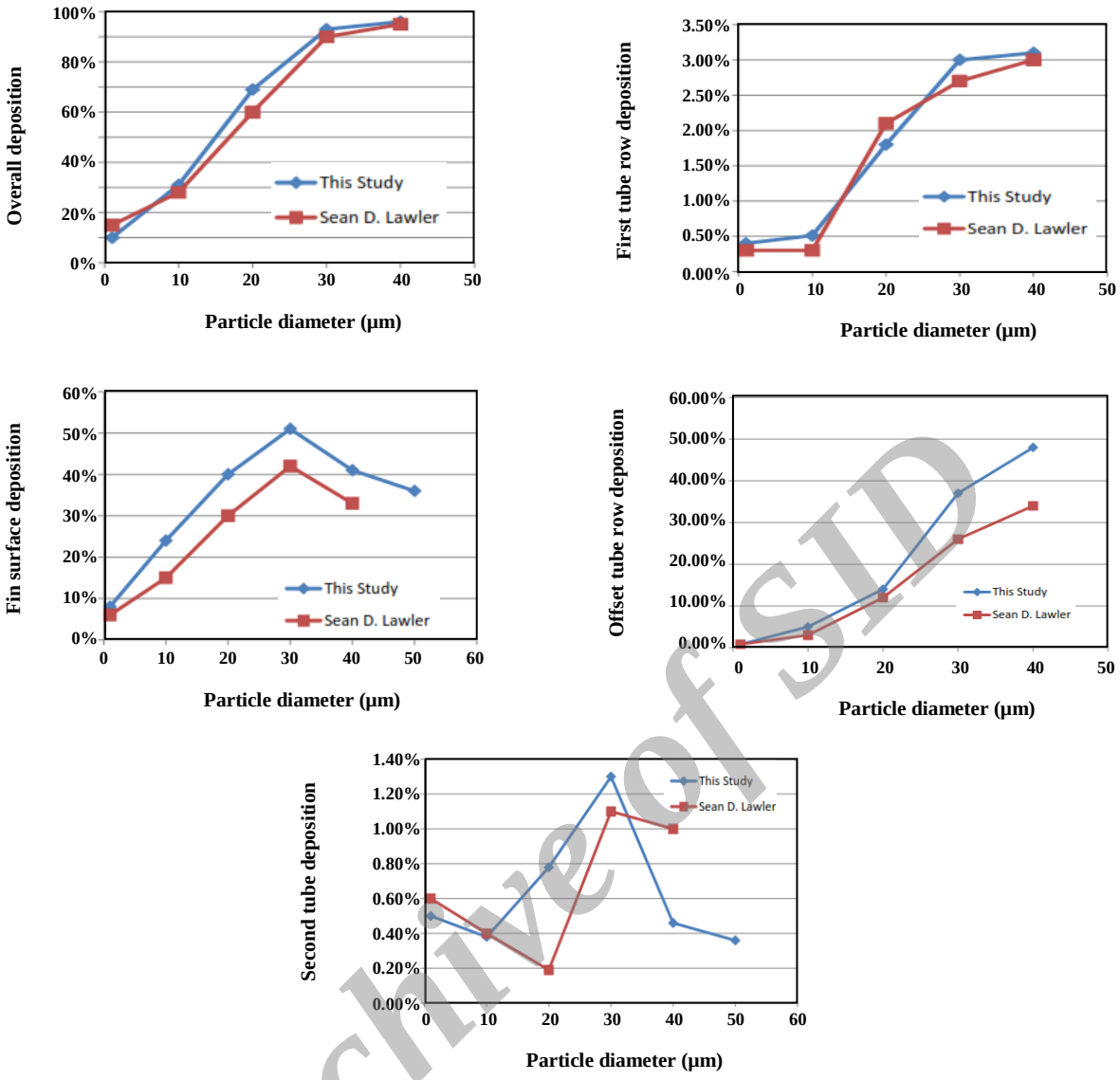

Fig. 3. Deposition rate versus particle diameter, (a) Overall deposition, (b) Fin surface deposition, (c) First tube row deposition, (d) Offset tube row deposition, (e) Second tube row deposition.

was injected to the inlet of domain as discrete phase [11]. Therefore the number of 1920 particles, due to the number of cells in the entrance of domain (YZ Plate), with the velocity and temperature of 1 m/s and 26.6 ^{0}C and various particle size distributions were injected to the inlet surface of domain as discrete phase. Lagrangian equations were applied for modeling dispersed phase. The turbulent intensity of 0.6% and length scale of 0.37 mm were calculated for the corresponding system. Due to the flow condition, low Reynolds number and wall functions, K-ω (SST) turbulence model preferred for running simulations. Buoyancy force, gravitational force, virtual mass force, thermophoreisis and Brownian diffusion are considered in all simulations as acting forces on the particles.

Validation of the results

For the purpose of validation, first the modeling was performed using single particle diameters of 1, 10, 20, 30 and 40 µm, injected in the domain at 26.6 ^{0}C with the air velocity of 1 m/s. The problem converged after running 6000 simulations, with residual values less than 10^{-4}. The results compared with the similar study of *Sean D. Lawler* [10] and found that similar compatibility as illustrated in Fig. 3.

Table 1: Particle size distribution in one of U.S Cities [12].

Diameter Range (μm)	Mass Fraction
0-1	0.20
1-5	0.13
5-10	0.25
10-20	0.22
20-30	0.11
30-40	0.09

Table 2: The values of Y_d, determined from the given data in Table 1.

Diameter, d (μm)	Mass Fraction with Diameter Greater than d, Y_d
1	0.80
5	0.67
10	0.42
20	0.20
30	0.09
40	0.00

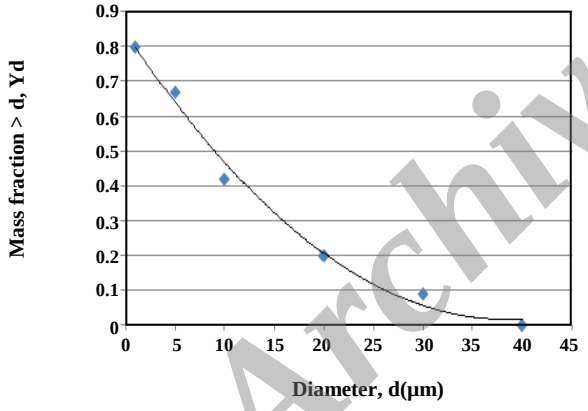

Fig. 4: Size distribution of particles.

Rosin-rammler method

This method is one of the Fluent option to analyze the effect of injecting various particle sizes simultaneously in the domain based on using linear equation. Based on Rosin-Rammler method and to calculate the deposition for various particle size distributions, a typical particle distribution in the environmental air of one of USA cities, shown in Table 1, is analyzed.

The distribution function of Rosin-Rammler is based on an exponential relationship between the particle diameter (d) and the mass fraction of particles with diameter greater than d as defined in Eq. (10), (Y_d);

$$Y_d = e^{-\left(d/\bar{d}\right)^n} \quad (10)$$

Where $\bar{d}$ is defined as the mean diameter and n as the spread parameter in Fluent.

From Table 1, the values of Y_d can be calculated and shown in Table 2.

From Eq. (10) while $d = \bar{d}$ the value of Y_d is obtained as below;

$Y_d = e^{-1} \approx 0.368$.

Fig. 5 also shows a plot of Y_d versus d. As seen, the value of $\bar{d}$ can be obtained from this figure where the value of Y_d is 0.368.

By observing the $\bar{d}$ value of 13.59 from Fig. 4, the value of n is obtained by substituting the data in Eq. (11).

$$n = \frac{\ln\left(-\ln Y_d\right)}{\ln\left(d/\bar{d}\right)} \quad (11)$$

An average value of *n*=0.463 is yielded from Eq. (11).

Turbulent dispersion of particles

Particles dispersion, due to fluid turbulency, could be tracked either by using "Stochastic Tracking" or "Cloud Tracking". In this study the turbulence effect on particulate deposition is investigated by stochastic tracking. The trajectory of particles are predicted using the mean phase velocity ($\bar{u}$) in trajectory equations. Furthermore the Random Walk Model (DRW) is applied for determining the instantaneous gas velocity [13].

$$u = u' + \bar{u} \quad (12)$$

The prediction includes the instantaneous fluctuating of turbulent velocity on particle trajectories. The number of tries is considered by inputting number 5 and activating DRW model option in the software.

RESULTS AND DISCUSSION

After running about 6000 particle tracking simulations and substituting the values in the software, the following results, shown through Figs. 5-15, can be obtained.

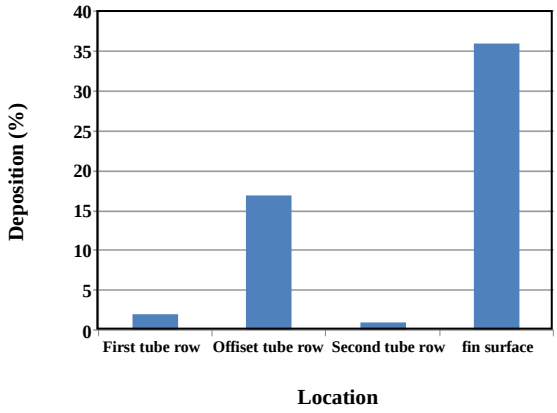

Fig. 5: Comparison of local deposition by Rosin-Rammler method.

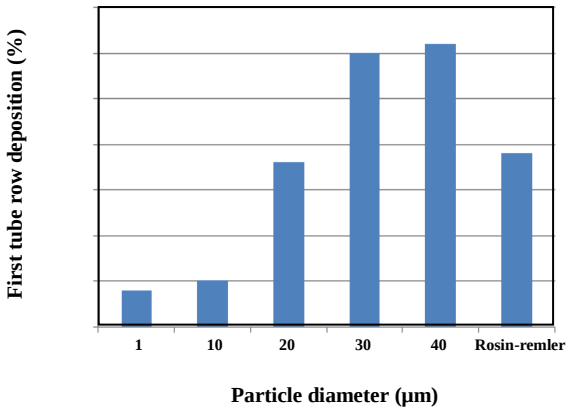

Fig. 8: Comparison of deposition on first tube row by Rosin-Rammler method with single particle diameter injection mode.

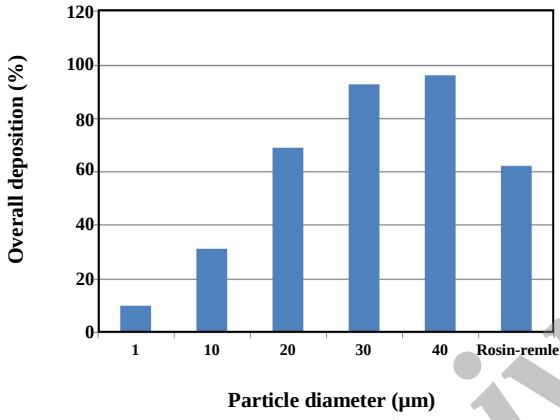

Fig. 6: Comparison of overall deposition by Rosin-Rammler method with single particle diameter injection mode.

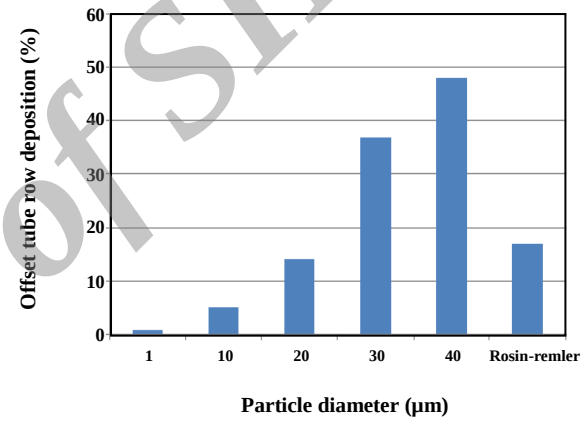

Fig. 9.: Comparison of deposition on offset tube row by Rosin-Rammler method with single particle diameter injection mode.

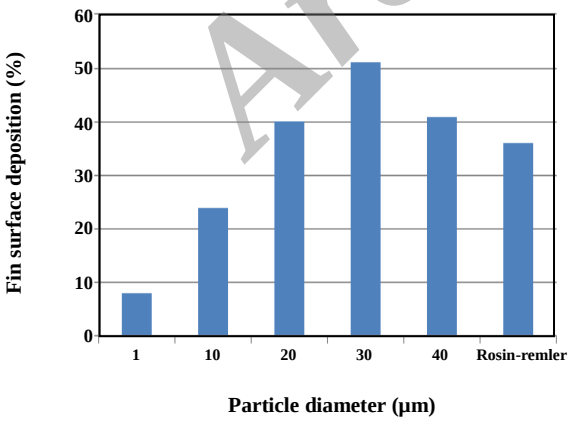

Fig. 7: Comparison of deposition on fin surface by Rosin-Rammler method with single particle diameter injection mode.

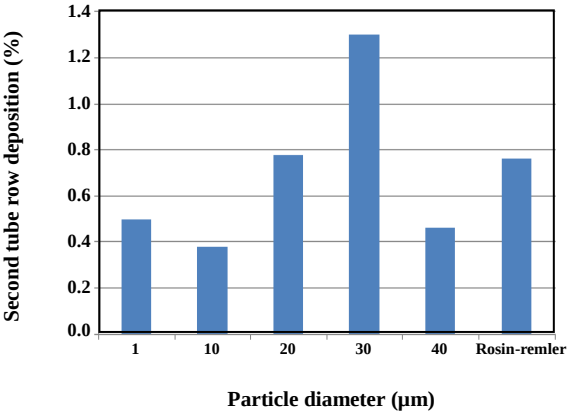

Fig. 10: Comparison of deposition on second tube row by Rosin-Rammler method with single particle diameter injection mode.

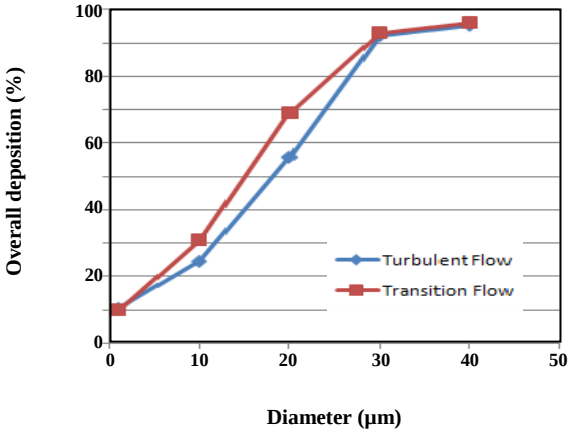

Fig. 11: Comparison of overall deposition.

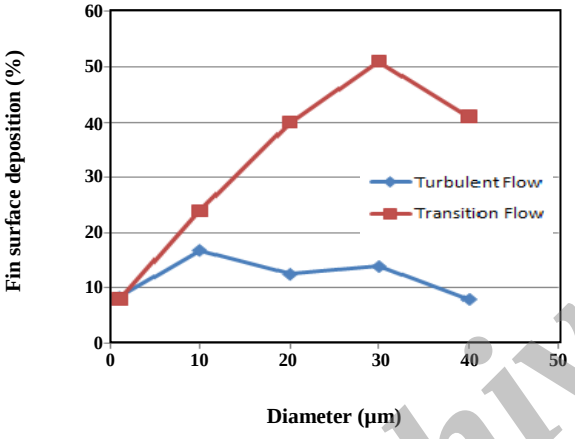

Fig. 12: Comparison of deposition rate on the fin surface.

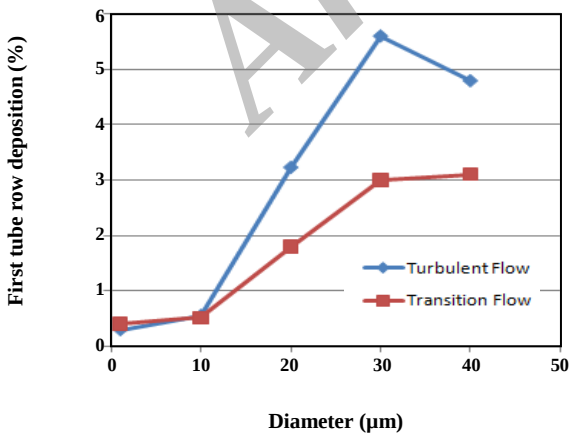

Fig. 13: Comparison of deposition rate on the first tube row.

Fig. 5 reveals that the majority of deposition, about 36%, occurs on the fin surface area. The offset tube row experiences higher deposition rates than the first and second tube rows.

As Figs. 6 to 10 show, deposition rate is highly affected by particle diameter. The greater particles, the higher deposition rates were occurred; this is due to the higher Stokes numbers of greater particles. From Fig. 6, it can be concluded that the overall deposition for particles over 30 µm exceeds from 90%. Furthermore the effect of gravity on greater particles leads to the higher deposition rates on the offset tube row. The deposition on the second tube row shows significant fluctuation because of the thermophoretic forces.

Deposition rate for particles less than 10 µm in diameter occurs on the downstream of domain due to trapping of particles in recirculation zone.

As shown through Figs. 6 to 10, deposition rate is considered based on various particle diameters that injected simultaneously in the domain. The analysis is performed with the corresponding mean diameter of particles. In the other word, the deposition in Rosin-Rammler method appears in the range of uniform particles deposition with diameter close to the mean diameter of analyzed air.

From Figs. 11 to 15 it is considered that fluid turbulency has not a significant effect on the deposition of particles less than 10 µm. In spite of considerably reduction on the deposition rate on the fin surface, the overall deposition can be reduced very slowly. In contrast, from Figs. 13 to 15, it can be found that turbulency could increase the deposition rates on the tubes of heat exchanger.

The contour plots of low Reynolds k-ω turbulence model for 10 µm particles with the velocity of 1 m/s are shown in Figs. 16 to 19.

Figs. 17 to 19 illustrate the contours of velocity magnitude, static pressure, static temperature and turbulent kinetic energy respectively.

It should be mentioned that the turbulent kinetic energy could be used to realize the fouling trend.

Fig. 16 shows the velocity magnitude contours of corresponding study while the flow injected to the domain with the velocity of 1 m/s. It should be mentioned that the velocity meets to its lowest magnitude in the domains behind the tubes. These domains are most capable for particle deposition.

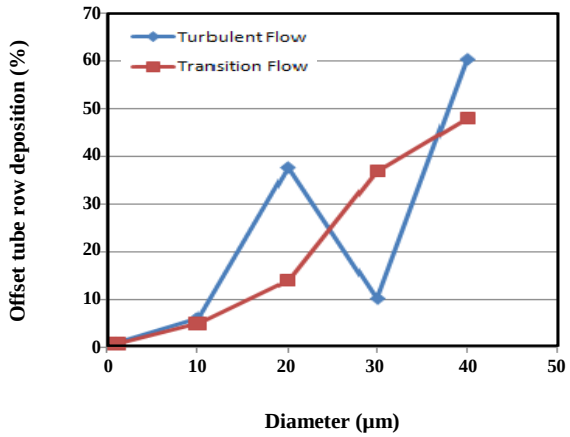

Fig. 14: Comparison of deposition rate on the offset tube row.

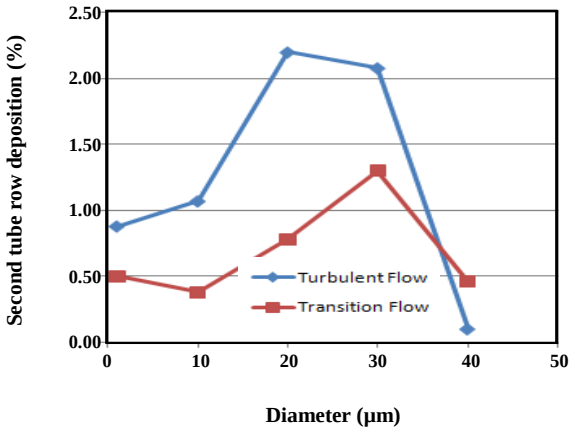

Fig. 15: Comparison of deposition rate on the second tube row.

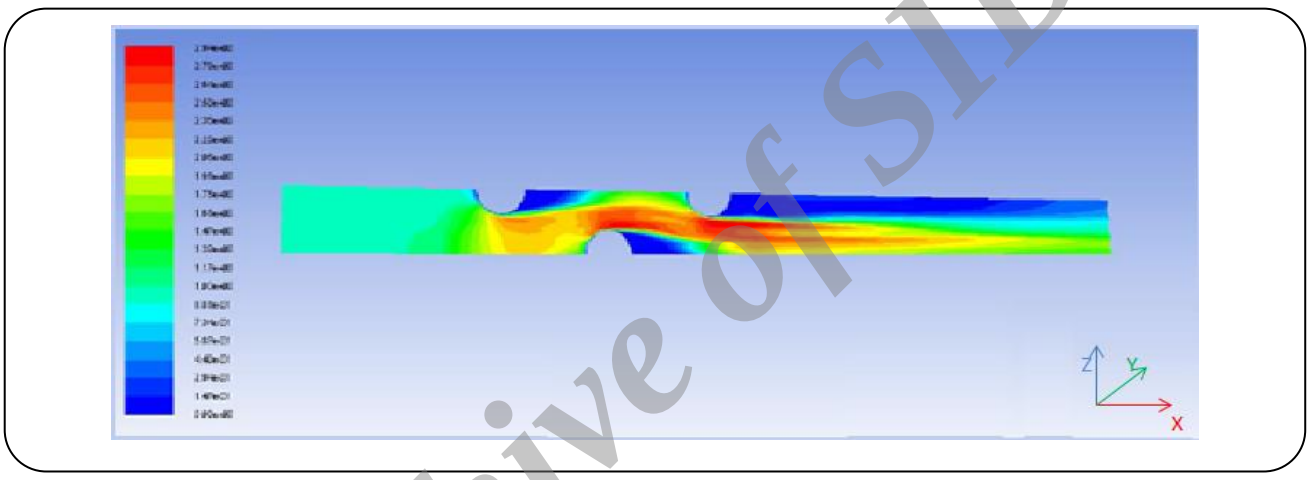

Fig. 16: Velocity magnitude contours plot.

Fig. 17 shows the pressure drop of the flow passing over the tubes. From Fig. 18, it can be concluded that the areas with the lowest temperature are most likely to experience the deposition of particles in this system.

CONCLUSIONS

A simulation was carried out by CFD analysis to study of particulate deposition on fin tube heat exchangers. The following results can be obtained:

1- Deposition rate is highly dependents on particle diameter rather than other parameters such as temperature in HVAC systems.

2- Fin surfaces were found to have the majority of particle deposition, while the least deposition occurs on first and second rows of tubes. The offset tube row experienced higher amount of deposition percentage. However deposition rates may vary due to different environmental particle size distributions.

3- The deposition rates calculated by Rosin-Rammler's method are near to mean diameter deposition rate in uniform particle diameter injection.

4- The turbulency not only results the higher pressure drops in the corresponding system, but also increases the deposition rate on the tubes of heat exchanger.

5- The larger particle diameter distribution leads to the higher particulate deposition rates.

Nomenclatures

Cs	Sutherland Constant
d	Diameter of Particles
$\bar{d}$	Mean Diameter of Particles
$F_{h,j}$	Diffusional Thermal Energy Flux in x_j Direction

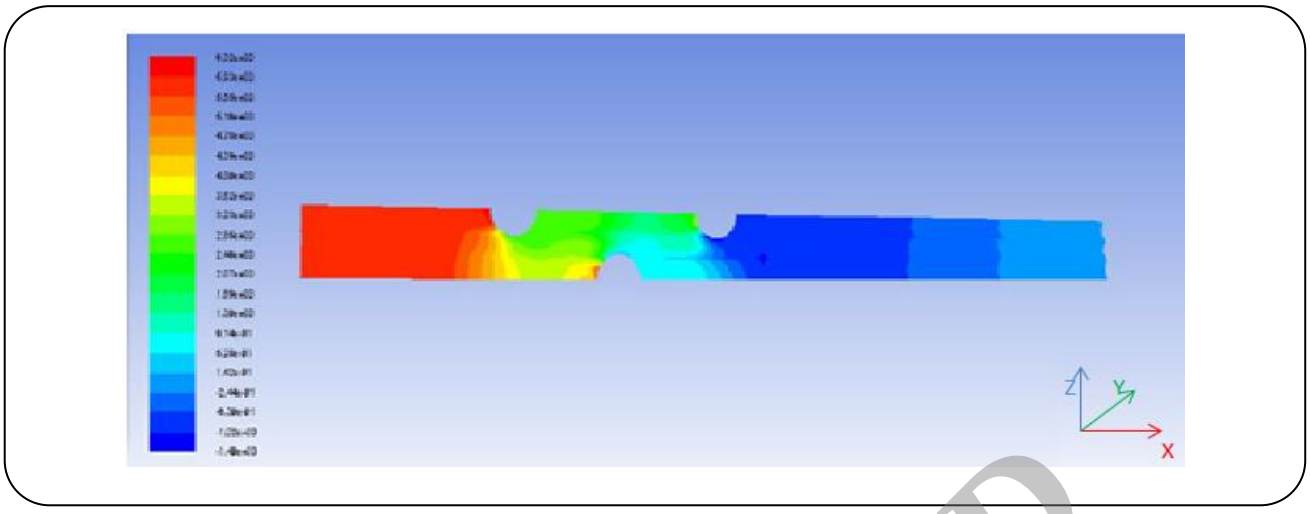

Fig. 17: Static pressure contour plot.

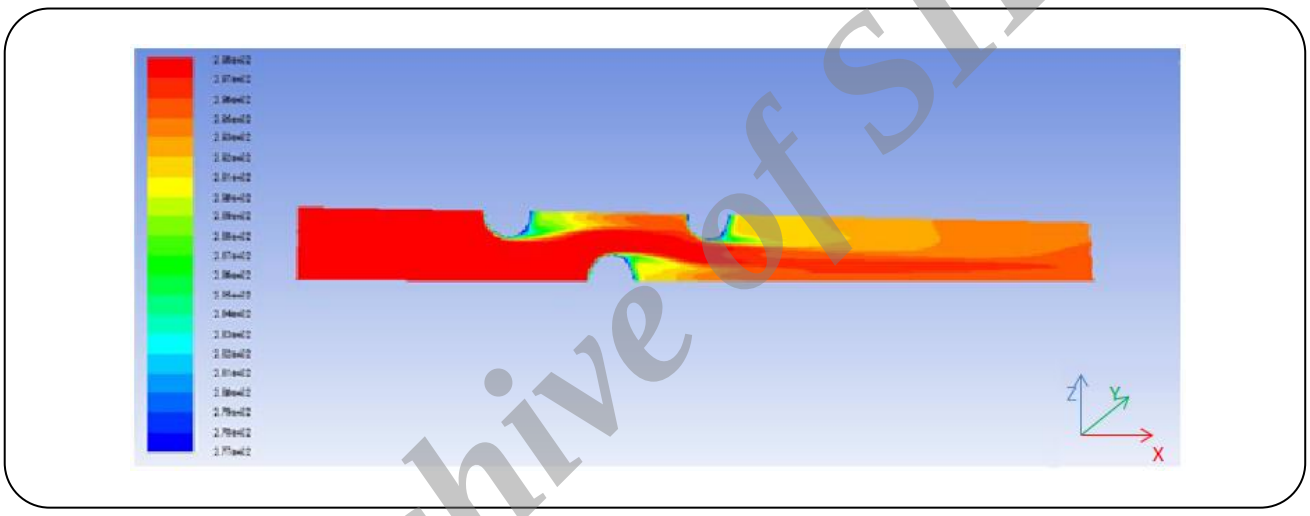

Fig. 18: Static temperature contours plot.

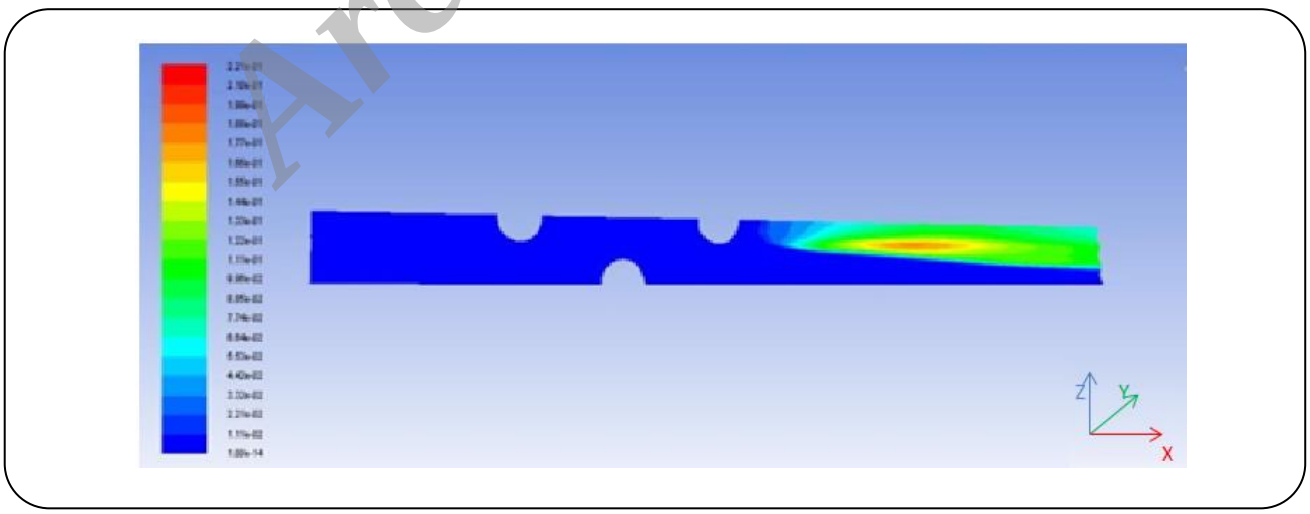

Fig. 19: Turbulent kinetic energy contours plot.

$F_{m,j}$	Diffusional Flux Component m in Direction x_j
H_m	Heat of Formation of constituent m
h_t	Thermal Enthalpy
k	Thermal Conductivity
M_m	Molecular Weight
n	Spread Parameter
R	Universal Gas Constant
$s_{c,m}$	Chemical Reaction Source Term
s_i	Momentum Source Term
s_h	Energy Source Term
S_m	Mass Source Term
T	Temperature
t	Time
$\bar{u}$	Mean Turbulent Velocity
Y_d	Mass Fraction of Particles with Diameter Greater than d
Y_m	Mass Fraction of Mixture Constituent m
μ	Viscosity
μ_0	Reference Viscosity
ρ	Density
$\tau_{i,j}$	Stress Tensor Components (Pa)

Received : Jan. 23, 2015 ; Accepted : May 11, 2015

REFERENCES

[1] Siegel J.A., "Particulate Fouling of HVAC Heat Exchangers", University of California, Berkeley, (2002).

[2] Jafari Nasr M.R., "Heat Exchanger Fouling", Research Institute of Petroleum Industry (RIPI) Publications Center, Iran (2011).

[3] Sun Y., Zhang Y., Baker D, Experimental Evaluation of Air-Side Particulate Fouling Performance Heat Exchanger, *ASHRAE Transactions*: 2-4 (2012).

[4] Siegel J.A., Nazaroff W.W., Predicting Particle Deposition on HVAC Heat Exchangers, *Elsevier Ltd.*: 2-4 (2003).

[5] McDowall R., "Fundamentals of HVAC Systems" Butterworth-Heinemann publications:19-23 (2006).

[6] Chuan Wang C., Recent Advances in Fin-and-Tube Heat Exchanger, *World Scientific. J. Air Conditioning & Refrigeration*; 3(2011).

[7] Laohalertdecha S., Dalkilic A.S., Wonfwises S., A Review on the Heat Transfer Performance and Pressure Drop Characteristics of Various Enhanced Tubes, *World Scientific. J. Air Conditioning & Refrigeration*: 5 (2012).

[8] Shah R.K., Sekulic D.P., "Fundamentals of Heat Exchanger design", John Wiley & Sons, Canada (2003).

[9] Gosman A.D., Developments in Industrial Computational Fluid Dynamics, *Trans. IChemE*, (1998).

[10] Lawler S.D., "Computational Study of Particle Deposition within a HVAC Heat Exchanger", Collage of Engineering and Computing of South California: 10-80 (2008).

[11] Jones J.W., Crawford R.H., Krishnan V., Vliet G.C., Wood, K.L., "Functional Model and Second Law Analysis Method for Energy Efficient Process Design: Applications in HVAC Systems Design", Vigain Harutunian Publications, The university of Texas at Austin: 6-10 (2003).

[12] Chow J.C., Watson J.G., "Guideline on Speculated Particulate Monitoring", Office of Air Quality Planning and Standards: 49 (1998).

[13] Fluent 6.3.26, User Guide, "Discrete Phase Models": CHP. 19 (2006) & "Overview and Limitations of the Discrete Phase Method": CHP 23(2006).